Chemical Engineering Science 134 (2015) 108–118

Contents lists available at ScienceDirect

Chemical Engineering Science

journal homepage: www.elsevier.com/locate/ces

Upscaling solute concentration transport equations of countercurrent dialyzer systems

Chen Yang [a], Qinglian Wang [a], Jiadong Guo [a], Akira Nakayama [b,c], Ting Qiu [a,*]

[a] School of Chemical Engineering, Fuzhou University, Fuzhou 350116, China
[b] Department of Mechanical Engineering, Shizuoka University, 3-5-1 Johoku, Hamamatsu 432-8561, Japan
[c] School of Civil Engineering and Architecture, Wuhan Polytechnic University, Wuhan 430023, Hubei, China

HIGHLIGHTS

- A general upscaled solute concentration transport model is proposed.
- The distribution coefficient is introduced into the upscaled model for the first time.
- The one-dimensional analysis is conducted for a hollow fiber dialyzer.
- The present analysis agrees well with experimental data and theoretical predictions.

ARTICLE INFO

Article history:
Received 29 November 2014
Received in revised form
25 February 2015
Accepted 16 April 2015
Available online 2 May 2015

Keywords:
Dialyzer
Upscaled model
Ultrafiltration
Volume averaging theory
Clearance enhancement

ABSTRACT

The present paper aims at an upscaled description of solute concentration transport processes in countercurrent dialyzer systems by means of a porous media approach based on the volume averaging theory. In consideration of solute diffusion and ultrafiltration processes, a general set of upscaled solute concentration transport equations has been derived for the three phases in a hollow fiber dialyzer, namely, the blood, membrane and dialysate phases. Moreover, the corresponding closure problems, which can be solved to obtain the effective properties in the upscaled model, are proposed. For the one-dimensional case, analytical expressions of solute concentrations in both blood and dialysate phases are achieved, so as to elucidate the influences of ultrafiltration flow rate and distribution coefficient on both clearance enhancement and solute concentration variations along the length of dialyzer. The results show that both ultrafiltration flow rate and distribution coefficient have no significant effects on solute concentration variations along the length of dialyzer. Nevertheless, the clearance enhancement are found to have linear relationship with both ultrafiltration flow rate and distribution coefficient.

1. Introduction

In the world, a considerable number of patients are suffering from renal failure. The patients can survive with the help of kidney replacement therapy. In kidney replacement therapy, the hollow fiber dialyzer widely used to remove metabolic wastes from blood, is a crucial device from the perspectives of economic aspects and patient's quality of life. Generally, fibers are made of ultrafiltration membranes and bundled inside the dialyzer. In order to evaluate, optimize and control various kinds of kidney replacement therapy, the development of mathematical models related to mass diffusion and ultrafiltration processes through membranes is highly needed.

In the literature, the Kedem and Katchalsky (1958) model was obtained appealing to the methods of the thermodynamics of irreversible processes, and successfully used to study the flow behavior in a semi-permeable membrane. Based on semi-infinite parallel-plate and cylindrical tube geometries, Cooney et al. (1974) presented theoretical analyses of mass transfer in hemodialyzers which contain blood and dialysate flowing streams separated by a semi-permeable membrane. Moreover, discussions associated with applications of the mathematical model to systems used in reality were also included. Palatý et al. (2006) proposed a simple yet reliable procedure to obtain the overall dialysis coefficient, permeability of the membrane and mass transfer coefficient of the membrane. In the above mentioned mathematical models, however, it should be noted that the impact of ultrafiltration was not taken into account.

In order to elucidate the ultrafiltration effects on a parallel-plate membrane dialysis module, Tu et al. (2006, 2009) conducted both theoretical and experimental studies, and claimed that a dialysis

* Corresponding author.
E-mail address: tingqiu@fzu.edu.cn (T. Qiu).

http://dx.doi.org/10.1016/j.ces.2015.04.037
0009-2509/

system coupled with ultrafiltration can sufficiently enhance the separation efficiency. Lu and Lu (2010) used a half-channel model to numerically simulate a sort of ultrafiltration problems. Tu and Ho (2010) developed a two-dimensional theoretical model of a flat-plate dialyzer with ultrafiltration operation, so as to investigate the influences of various parameters, such as retentate phase flow rate, dialysate flow rate, ultrafiltration flow rate and channel thickness ratio, on both mass transfer rate and concentration distribution. The interested reader could refer to Waniewski (2006) for an excellent review with regarding to mathematical modeling of fluid flow and solute transport in hemodialysis and peritoneal dialysis.

The aforementioned studies on modeling hollow fiber dialyzers were conducted based on an individual fiber that was assumed to represent the whole bundle. But this assumption is only valid when each fiber in the system is identical. Thus, there are a few numerical attempts made to simulate the fluid and solute transport processes in hollow fiber dialyzers consisting of thousands of fibers (Kumar and Upadhyay, 2000; Shirazian et al., 2009). Due to the difficulties to resolve the details of fluid flow and solute concentration transport within the dialyzer, the corresponding computations are quite challenging. To overcome these limitations, porous media approach based on the volume averaging theory are used and have proven to be suitable (Labecki et al., 1995; Sano et al., 2013).

Ding et al. (2004) treated a hollow fiber bundle as a porous media region which is composed of two interpenetrating porous flow regions, and achieved a double porous media for mass transfer of hollow fiber hemodialyzers, which was validated by comparing with experimental data. By exploiting a porous media approach, Wang et al. (2010) numerically studied the hydrodynamic conditions of membrane filtration zone of a full-scale submerged hollow fiber system. More recently, Sano and Nakayama (2012) derived a general set of macroscopic governing equations for three phases in a hollow fiber membrane dialyzer after a rigorous mathematical development based on the volume averaging theory. Furthermore, a set of governing parameter of dialyzer system were identified and an analytical expression for the solute clearance was presented for the one-dimensional case. In this Sano–Nakayama membrane transport model, the effect of the reflection coefficient was not taken into consideration. Subsequently, Nakayama and Sano (2013) extended the Sano–Nakayama membrane transport model by introducing the reflection coefficient into the set of macroscopic governing equations and applied it to analyze the concentration polarization phenomena with respect to hollow fiber reverse osmosis desalination systems. However, some terms and parameters, such as conductive and non-traditional convective transport terms, as well as distribution coefficient, are still missing in the new general set of macroscopic governing equations for three phases in a hollow fiber membrane dialyzer.

In the present paper, we shall revisit the fluid flow and solute concentration transport in countercurrent dialyzer systems, and derive the upscaled governing equations based on the volume averaging theory on the basis of Quintard and Whitaker (1993). Then, for the one-dimensional case, the upscaled governing equations are reduced, so as to investigate the effects of ultrafiltration flow rate and distribution coefficient on both solute concentration variations along the axial coordinate and clearance enhancement. Eventually, the present model proposed for the countercurrent dialyzer systems are validated by comparing the results against available experimental data and theoretical predictions.

2. Upscaling procedures

Hollow fiber dialyzers consist of a bundle of hollow fibers of ultrafiltration membranes, which are able to remove metabolic wastes carried by the blood. The schematic structure illustrated in Fig. 1 is commonly used to study hemodialysis process in the literature. Such individual fiber unit is called Krogh cylinder, since Krogh (1919) performed the pioneer modeling research on capillaries in tissue which are treated as the same multi-fiber geometry. During hemodialysis process, blood and dialysate separated by permeable porous membranes flow in the countercurrent pattern. Furthermore, they exchange solute contents through the permeable porous membranes in which ultrafiltration takes place.

As proposed by Sano and Nakayama (2012), the microscopic governing equations for countercurrent dialyzer systems are presented as follows,

$$\nabla \cdot \mathbf{V} = 0 \tag{1}$$

$$\rho \frac{\partial \mathbf{V}}{\partial t} + \rho \nabla \cdot (\mathbf{V}\mathbf{V}) = -\nabla p + \mu \nabla^2 \mathbf{V} \tag{2}$$

$$\frac{\partial c}{\partial t} + \nabla \cdot (\mathbf{V} c) = \nabla \cdot (D \nabla c) \tag{3}$$

The interfacial boundary conditions of solute concentration are

$$r = d_b/2: \quad c_b = c_m \tag{4a}$$

and

$$-\mathbf{n}_{bm} \cdot (D_b \nabla c_b - \mathbf{V}_b c_b) = -\mathbf{n}_{bm} \cdot D_m \nabla c_m \tag{4b}$$

$$r = d_d/2: \quad c_d = c_m \tag{5a}$$

and

$$-\mathbf{n}_{dm} \cdot (D_d \nabla c_d - \mathbf{V}_d c_d) = -\mathbf{n}_{dm} \cdot D_m \nabla c_m \tag{5b}$$

where the subscripts b, m, d will refer to the blood, membrane and dialysate phases, respectively.

The upscaling process involves many steps that have been discussed at length in the literature. In this study, the details for the most well-known aspects, which can be found in Whitaker (1999) for the associated discussion, will not be provided. Macroscale variables are defined over the representative elementary volume (REV: Bear, 1972) sketched in Fig. 2 as

$$\langle \psi_f \rangle = \frac{1}{V} \int_{V_f} \psi_f dV \tag{6a}$$

$$\langle \psi_f \rangle^f = \frac{1}{V_f} \int_{V_f} \psi_f dV \tag{6b}$$

$$\langle \psi_f \rangle = \varepsilon_f \langle \psi_f \rangle^f \tag{7}$$

where

$$\varepsilon_f = V_f/V \tag{8}$$

Based on the physical model shown in Fig. 1, the following parameters existing in the upscaled model are given by

$$\varepsilon_b = \frac{N \pi d_b^2/4}{A} \tag{9a}$$

$$\varepsilon_m = 4\frac{t_m}{d_b}\left(1 + \frac{t_m}{d_b}\right)\varepsilon_b \tag{9b}$$

$$\varepsilon_d = 1 - \left[1 + 4\frac{t_m}{d_b}\left(1 + \frac{t_m}{d_b}\right)\right]\varepsilon_b \tag{9c}$$

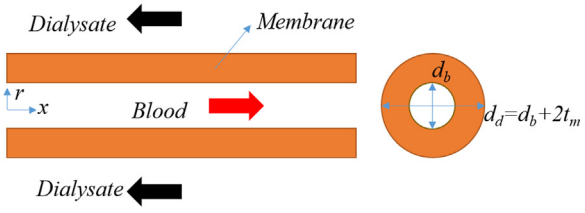

Fig. 1. The structure of dialyzer system.

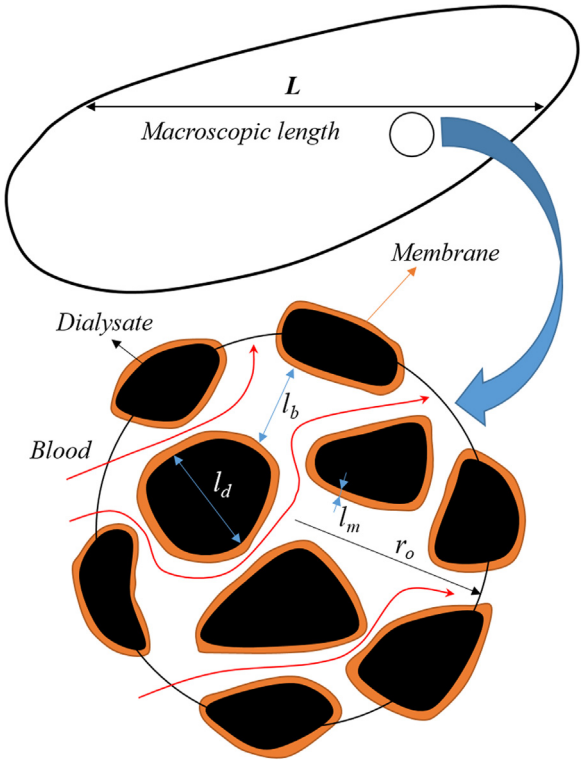

Fig. 2. Averaging volume in the representative elementary volume (REV).

$$a_b = \frac{4\varepsilon_b}{d_b} \tag{9d}$$

$$a_d = \frac{4\varepsilon_b}{d_b}\left(1+2\frac{t_m}{d_b}\right) \tag{9e}$$

where ε_b, ε_d and ε_m are the volume fractions of blood, dialysate and membrane phases, a_b and a_d are the specific surface areas of the blood compartment and the dialysate compartment, respectively. Moreover, N is the number of hollow fibers, A is the cross-sectional area of the dialyzer structure, d_b, d_d and t_m are the inner, outer diameters of the hollow fiber and membrane thickness, respectively.

In addition, the local phase variables are related to the intrinsic phase averages and their corresponding deviations based on Gray (1975)'s spatial decomposition shown as follows

$$\mathbf{V}_f = \langle \mathbf{V}_f \rangle^f + \tilde{\mathbf{V}}_f, \tag{10a}$$

$$p_f = \langle p_f \rangle^f + \tilde{p}_f \tag{10b}$$

$$c_f = \langle c_f \rangle^f + \tilde{c}_f \tag{10c}$$

First, we will treat the continuity and momentum equations. Since the derivations of macroscale continuity and momentum equations have been shown in Sano and Nakayama (2012), the present paper is devoted to deriving the upscaled solute concentration transport equations for three phases in a hollow fiber dialyzer, namely, the blood, membrane and dialysate phases. All subsequent developments will make use of the assumption of scale separation, usually expressed as $l_b, l_m, l_d \ll r_o \ll L$. Hence, the macroscopic solute transport equations of three phases may be given as follows

$$\frac{\partial \varepsilon_b \langle c_b \rangle^b}{\partial t} + \nabla \cdot \left(\varepsilon_b \langle \mathbf{V}_b \rangle^b \langle c_b \rangle^b \right) = \nabla \cdot \left[D_b \left(\varepsilon_b \nabla \langle c_b \rangle^b + \frac{1}{V}\int_{A_{bm}} \mathbf{n}_{bm} \tilde{c}_b dA \right) \right]$$
$$- \nabla \cdot \left\langle \tilde{\mathbf{V}}_b \tilde{c}_b \right\rangle + \frac{1}{V}\int_{A_{bm}} \mathbf{n}_{bm} \cdot D_b \nabla c_b dA - \frac{1}{V}\int_{A_{bm}} \mathbf{n}_{bm} \cdot \mathbf{V}_b c_b dA \tag{11}$$

$$\frac{\partial \varepsilon_m \langle c_m \rangle^m}{\partial t} = \nabla \cdot \left[D_m \left(\varepsilon_m \nabla \langle c_m \rangle^m + \frac{1}{V}\int_{A_{mb}} \mathbf{n}_{mb} \tilde{c}_m dA + \frac{1}{V}\int_{A_{md}} \mathbf{n}_{md} \tilde{c}_m dA \right) \right]$$
$$+ \frac{1}{V}\int_{A_{mb}} \mathbf{n}_{mb} \cdot D_m \nabla c_m dA + \frac{1}{V}\int_{A_{md}} \mathbf{n}_{md} \cdot D_m \nabla c_m dA \tag{12}$$

$$\frac{\partial \varepsilon_d \langle c_d \rangle^d}{\partial t} + \nabla \cdot \left(\varepsilon_d \langle \mathbf{V}_d \rangle^d \langle c_d \rangle^d \right) = \nabla \cdot \left[D_d \left(\varepsilon_d \nabla \langle c_d \rangle^d + \frac{1}{V}\int_{A_{dm}} \mathbf{n}_{dm} \tilde{c}_d dA \right) \right]$$
$$- \nabla \cdot \left\langle \tilde{\mathbf{V}}_d \tilde{c}_d \right\rangle + \frac{1}{V}\int_{A_{dm}} \mathbf{n}_{dm} \cdot D_d \nabla c_d dA - \frac{1}{V}\int_{A_{dm}} \mathbf{n}_{dm} \cdot \mathbf{V}_d c_d dA \tag{13}$$

According to the upscaled continuity equation of blood phase obtained by Sano and Nakayama (2012), we can get the following equation

$$\nabla \cdot \varepsilon_b \langle \mathbf{V}_b \rangle^b = -\frac{1}{V}\int_{A_{bm}} \mathbf{n}_{bm} \mathbf{V}_b dA = -a_b J_V = -\omega \tag{14}$$

where ω is the perfusion rate, which is the product of the specific area a_b and ultrafiltration velocity J_V. In what follows, the macroscopic solute transport equation of blood phase can be further simplified and written as below

$$\frac{\partial \varepsilon_b \langle c_b \rangle^b}{\partial t} + \langle \mathbf{V}_b \rangle^b \cdot \nabla \left(\varepsilon_b \langle c_b \rangle^b \right) = \nabla \cdot \left[D_b \left(\varepsilon_b \nabla \langle c_b \rangle^b + \frac{1}{V}\int_{A_{bm}} \mathbf{n}_{bm} \tilde{c}_b dA \right) \right] -$$
$$\nabla \cdot \left\langle \tilde{\mathbf{V}}_b \tilde{c}_b \right\rangle + \frac{1}{V}\int_{A_{bm}} \mathbf{n}_{bm} \cdot D_b \nabla \tilde{c}_b dA - \frac{1}{V}\int_{A_{bm}} \mathbf{n}_{bm} \cdot \mathbf{V}_b \tilde{c}_b dA \tag{15}$$

In order to close this equation, we need to 1) develop balance equations for the solute concentration deviation $\tilde{c}_b$, and 2) express the deviation as functions of macroscopic concentration. By subtracting the microscale equation from the macroscale unclosed forms and using decomposition definitions, we can obtain deviation equation for solute concentration of blood phase. Furthermore, the governing equation of the spatial deviation for solute concentration of blood phase can be further simplified on the basis of the following restrictions ($l_b, l_m, l_d \ll L$)

$$\nabla \cdot (D_b \nabla \tilde{c}_b) \gg \varepsilon_b^{-1} \nabla \cdot \left(\frac{D_b}{V}\int_{A_{bm}} \mathbf{n}_{bm} \tilde{c}_b dA \right) \tag{16a}$$

$$\mathbf{v}_b \cdot \nabla \tilde{c}_b \gg \varepsilon_b^{-1} \nabla \cdot (\tilde{\mathbf{v}}_b \tilde{c}_b) \tag{16b}$$

Therefore, the simplified governing equation of the spatial deviation for solute concentration of blood phase are obtained and indicated as below

$$\frac{\partial \tilde{c}_b}{\partial t} + \mathbf{V}_b \cdot \nabla \tilde{c}_b + \tilde{\mathbf{V}}_b \cdot \nabla \langle c_b \rangle^b = \nabla (D_b \nabla \tilde{c}_b)$$
$$- \frac{\varepsilon_b^{-1}}{V}\int_{A_{bm}} \mathbf{n}_{bm} \cdot D_b \nabla \tilde{c}_b dA + \frac{\varepsilon_b^{-1}}{V}\int_{A_{bm}} \mathbf{n}_{bm} \cdot \mathbf{V}_b \tilde{c}_b dA \tag{17}$$

By analogy with the preceding procedures, the simplified governing equations of the spatial deviations for solute concentrations of both membrane and dialysate phases are obtained.

$$\frac{\partial \tilde{c}_m}{\partial t} = \nabla (D_m \nabla \tilde{c}_m) - \frac{\varepsilon_m^{-1}}{V}\int_{A_{mb}} \mathbf{n}_{mb} \cdot D_m \nabla \tilde{c}_m dA - \frac{\varepsilon_m^{-1}}{V}\int_{A_{md}} \mathbf{n}_{md} \cdot D_m \nabla \tilde{c}_m dA \tag{18}$$

$$\frac{\partial \tilde{c}_d}{\partial t} + \mathbf{V}_d \cdot \nabla \tilde{c}_d + \tilde{\mathbf{V}}_d \cdot \nabla \langle c_d \rangle^d = \nabla (D_d \nabla \tilde{c}_d)$$
$$- \frac{\varepsilon_d^{-1}}{V}\int_{A_{dm}} \mathbf{n}_{dm} \cdot D_d \nabla \tilde{c}_d dA + \frac{\varepsilon_d^{-1}}{V}\int_{A_{dm}} \mathbf{n}_{dm} \cdot \mathbf{V}_d \tilde{c}_d dA \tag{19}$$

We assume the closure problem to be quasi-steady. If one wants to retain all of the dynamics of the coupling, a closure may be introduced involving time convolution products (Moyne, 1997; Davit et al., 2012). As shown in Davit et al. (2012), the time convolutions, after some relaxation time, may be approximated by a quasi-steady closure which plays a fundamental role in the discussion concerning the various macroscale models. In this paper, we will use such a closure. Therefore, the governing equations of the spatial deviations for solute concentrations of three phases shown in Eqs. (17)–(19) can be further reduced as follows

$$\mathbf{V}_b\cdot\nabla\tilde{c}_b+{}_b\cdot\nabla\langle c_b\rangle^b{}_{Source}=\nabla(D_b\nabla\tilde{c}_b)$$
$$-\frac{\varepsilon_b^{-1}}{V}\int_{A_{bm}}\mathbf{n}_{bm}\cdot D_b\nabla\tilde{c}_b dA+\frac{\varepsilon_b^{-1}}{V}\int_{A_{bm}}\mathbf{n}_{bm}\cdot\mathbf{V}_b\tilde{c}_b dA \tag{20}$$

$$0=\nabla(D_m\nabla\tilde{c}_m)-\frac{\varepsilon_m^{-1}}{V}\int_{A_{mb}}\mathbf{n}_{mb}\cdot D_m\nabla\tilde{c}_m dA-\frac{\varepsilon_m^{-1}}{V}\int_{A_{md}}\mathbf{n}_{md}\cdot D_m\nabla\tilde{c}_m dA \tag{21}$$

$$\mathbf{V}_d\cdot\nabla\tilde{c}_d+{}_d\cdot\nabla\langle c_d\rangle^d{}_{Source}=\nabla(D_d\nabla\tilde{c}_d)$$
$$-\frac{\varepsilon_d^{-1}}{V}\int_{A_{dm}}\mathbf{n}_{dm}\cdot D_d\nabla\tilde{c}_d dA+\frac{\varepsilon_d^{-1}}{V}\int_{A_{dm}}\mathbf{n}_{dm}\cdot\mathbf{V}_d\tilde{c}_d dA \tag{22}$$

Correspondingly, the interfacial boundary conditions are expressed as follows

$$r=d_b/2:\qquad \tilde{c}_b=\tilde{c}_m+\underbrace{\left(\langle c_m\rangle^m-\langle c_b\rangle^b\right)}_{Source} \tag{23a}$$

$$\underbrace{-\mathbf{n}_{dm}\cdot D_d\nabla\langle c_d\rangle^d}_{Source}-\mathbf{n}_{bm}\cdot D_b\nabla\tilde{c}_b+\underbrace{\mathbf{n}_{bm}\cdot V_b\langle c_b\rangle^b}_{Source}+\mathbf{n}_{bm}\cdot\mathbf{V}_b\tilde{c}_b=\underbrace{-\mathbf{n}_{dm}\cdot D_m\nabla\langle c_m\rangle^m}_{Source}-\mathbf{n}_{bm}\cdot D_m\nabla\tilde{c}_m \tag{23b}$$

$$r=d_d/2:\quad \tilde{c}_d=\tilde{c}_m+\underbrace{\left(\langle c_m\rangle^m-\langle c_d\rangle^d\right)}_{Source} \tag{24a}$$

$$\underbrace{-\mathbf{n}_{dm}\cdot D_d\nabla\langle c_d\rangle^d}_{Source}-\mathbf{n}_{dm}\cdot D_d\nabla\tilde{c}_d+\underbrace{\cdot\mathbf{V}_d\langle c_d\rangle^d}_{Source}+\mathbf{n}_{dm}\cdot\mathbf{V}_d\tilde{c}_d=\underbrace{-\mathbf{n}_{dm}\cdot D_m\nabla\langle c_m\rangle^m}_{Source}-\mathbf{n}_{dm}\cdot D_m\nabla\tilde{c}_m \tag{24b}$$

Furthermore, we can make use of the mass flux boundary conditions given in Eqs. (23b) and (24b) to show that these interfacial area integrals indicated in Eqs. (17)–(19) are related by

$$\tfrac{1}{V}\textstyle\int_{A_{bm}}\mathbf{n}_{bm}\cdot D_b\nabla\tilde{c}_b dA-\tfrac{1}{V}\int_{A_{bm}}\mathbf{n}_{bm}\cdot\mathbf{V}_b\tilde{c}_b dA+\tfrac{1}{V}\int_{A_{mb}}\mathbf{n}_{mb}\cdot D_m\nabla\tilde{c}_m dA=\frac{1}{V}\int_{A_{bm}}\mathbf{n}_{bm}\cdot\mathbf{V}_b\langle c_b\rangle^b dA=\omega\langle c_b\rangle^b=q_{bm} \tag{25}$$

$$\tfrac{1}{V}\textstyle\int_{A_{dm}}\mathbf{n}_{dm}\cdot D_d\nabla\tilde{c}_d dA-\tfrac{1}{V}\int_{A_{dm}}\mathbf{n}_{dm}\cdot\mathbf{V}_d\tilde{c}_d dA+\tfrac{1}{V}\int_{A_{md}}\mathbf{n}_{md}\cdot D_m\nabla\tilde{c}_m dA=\frac{1}{V}\int_{A_{dm}}\mathbf{n}_{dm}\cdot\mathbf{V}_d\langle c_d\rangle^d dA=-\omega\langle c_d\rangle^d=q_{dm} \tag{26}$$

Given these source terms indicated in the closure problems, the following representations for $\tilde{c}_b$, $\tilde{c}_m$ and $\tilde{c}_d$ are suggested by Quintard and Whitaker (2000)

$$\tilde{c}_b=\mathbf{b}_{bb}\cdot\nabla\langle c_b\rangle^b+\mathbf{b}_{bm}\cdot\nabla\langle c_m\rangle^m+s_b\left(\langle c_m\rangle^m-\langle c_b\rangle^b\right)+r_{bm}q_{bm} \tag{27a}$$

$$\tilde{c}_m=\mathbf{b}_{mm}\cdot\nabla\langle c_m\rangle^m+\mathbf{b}_{mb}\cdot\nabla\langle c_b\rangle^b+\mathbf{b}_{md}\cdot\nabla\langle c_d\rangle^d+s_{mb}\left(\langle c_m\rangle^m-\langle c_b\rangle^b\right)+s_{md}\left(\langle c_m\rangle^m-\langle c_d\rangle^d\right)+q_{bm}+r_{md}q_{dm} \tag{27b}$$

$$\tilde{c}_d=\mathbf{b}_{dd}\cdot\nabla\langle c_d\rangle^d+\mathbf{b}_{dm}\cdot\nabla\langle c_m\rangle^m+s_d\left(\langle c_m\rangle^m-\langle c_d\rangle^d\right)+r_{dm}q_{dm} \tag{27c}$$

where $\mathbf{b}_{bb}$, $\mathbf{b}_{bm}$, $\mathbf{b}_{mm}$, $\mathbf{b}_{mb}$, $\mathbf{b}_{md}$, $\mathbf{b}_{dd}$, $\mathbf{b}_{dm}$, s_b, s_{mb}, s_{md} and s_d are closure variables. Moreover, r_{bm}, r_{mb}, r_{dm} and r_{md} are the specific closure variables for the interfacial mass flux of adjacent two phases, which determine how the interfacial mass flux is distributed between the adjacent two phases.

All the associated closure problems are presented in the Appendix. After solving the associated closure problems, we can obtain the closed form of macroscopic governing equations given by

$$\frac{\partial\varepsilon_b\langle c_b\rangle^b}{\partial t}+\nabla\cdot\left(\varepsilon_b\langle\mathbf{V}_b\rangle^b\langle c_b\rangle^b\right)=\nabla\cdot\left[\mathbf{D}_{bb}\cdot\nabla\langle c_b\rangle^b+\mathbf{D}_{bm}\cdot\nabla\langle c_m\rangle^m\right]+\nabla\cdot\left(\mathbf{u}_b\left(\langle c_m\rangle^m-\langle c_b\rangle^b\right)\right)+\mathbf{u}_{bb}\cdot\nabla\langle c_b\rangle^b+\mathbf{u}_{bm}\cdot\nabla\langle c_m\rangle^m-a_bh_{mb}\left(\langle c_b\rangle^b-\langle c_m\rangle^m\right)-\xi_{mb}\omega\langle c_b\rangle^b \tag{28}$$

$$\frac{\partial\varepsilon_m\langle c_m\rangle^m}{\partial t}=\nabla\cdot\left[\mathbf{D}_{mm}\cdot\nabla\langle c_m\rangle^m+\mathbf{D}_{mb}\cdot\nabla\langle c_b\rangle^b+\mathbf{D}_{md}\cdot\nabla\langle c_d\rangle^d\right]+\nabla\cdot\left(\mathbf{u}_{m1}\left(\langle c_m\rangle^m-\langle c_b\rangle^b\right)\right)+\nabla\cdot\left(\mathbf{u}_{m2}\left(\langle c_m\rangle^m-\langle c_d\rangle^d\right)\right)+\mathbf{u}_{mm}\cdot\nabla\langle c_m\rangle^m+\mathbf{u}_{mb}\cdot\nabla\langle c_b\rangle^b+\mathbf{u}_{md}\cdot\nabla\langle c_d\rangle^d+a_bh_{mb}\left(\langle c_b\rangle^b-\langle c_m\rangle^m\right)+a_dh_{md}\left(\langle c_d\rangle^d-\langle c_m\rangle^m\right)+\xi_{mb}\omega\langle c_b\rangle^b-\xi_{md}\omega\langle c_d\rangle^d \tag{29}$$

$$\frac{\partial\varepsilon_d\langle c_d\rangle^d}{\partial t}+\nabla\cdot\left(\varepsilon_d\langle\mathbf{V}_d\rangle^d\langle c_d\rangle^d\right)=\nabla\cdot\left[\mathbf{D}_{dd}\cdot\nabla\langle c_d\rangle^d+\mathbf{D}_{dm}\cdot\nabla\langle c_m\rangle^m\right]+\nabla\cdot\left(\mathbf{u}_d\left(\langle c_m\rangle^m-\langle c_d\rangle^d\right)\right)+\mathbf{u}_{dd}\cdot\nabla\langle c_d\rangle^d+\mathbf{u}_{dm}\cdot\nabla\langle c_m\rangle^m-a_dh_{md}\left(\langle c_d\rangle^d-\langle c_m\rangle^m\right)+\xi_{md}\omega\langle c_d\rangle^d \tag{30}$$

Note that the effective transport coefficients are defined by

$$\mathbf{D}_{bb}=\varepsilon_bD_b\mathbf{I}+\frac{1}{V}\int_{A_{bm}}\mathbf{n}_{bm}\mathbf{b}_{bb}dA-\left\langle\tilde{\mathbf{V}}_b\mathbf{b}_{bb}\right\rangle \tag{31a}$$

$$\mathbf{D}_{bm}=\frac{1}{V}\int_{A_{bm}}\mathbf{n}_{bm}\mathbf{b}_{bm}dA-\left\langle\tilde{\mathbf{V}}_b\mathbf{b}_{bm}\right\rangle \tag{31b}$$

$$\mathbf{D}_{mm}=\varepsilon_mD_m\mathbf{I}+\frac{1}{V}\int_{A_{mb}}\mathbf{n}_{mb}\mathbf{b}_{mm}dA+\frac{1}{V}\int_{A_{md}}\mathbf{n}_{md}\mathbf{b}_{mm}dA \tag{31c}$$

$$\mathbf{D}_{mb}=\frac{1}{V}\int_{A_{mb}}\mathbf{n}_{mb}\mathbf{b}_{mb}dA \tag{31d}$$

$$\mathbf{D}_{md}=\frac{1}{V}\int_{A_{md}}\mathbf{n}_{md}\mathbf{b}_{md}dA \tag{31e}$$

$$\mathbf{D}_{dd}=\varepsilon_dD_d\mathbf{I}+\frac{1}{V}\int_{A_{dm}}\mathbf{n}_{dm}\mathbf{b}_{dd}dA-\left\langle\tilde{\mathbf{V}}_d\mathbf{b}_{dd}\right\rangle \tag{31f}$$

$$\mathbf{D}_{dm}=\frac{1}{V}\int_{A_{dm}}\mathbf{n}_{dm}\mathbf{b}_{dm}dA-\left\langle\tilde{\mathbf{V}}_d\mathbf{b}_{dm}\right\rangle \tag{31g}$$

In addition, the mass transfer coefficients are given by

$$a_bh_{mb}=\frac{1}{V}\int_{A_{bm}}\mathbf{n}_{bm}\cdot D_b\nabla s_bdA-\frac{1}{V}\int_{A_{bm}}\mathbf{n}_{bm}\cdot\mathbf{V}_bs_bdA$$

$$= -\frac{1}{V}\int_{A_{mb}} \mathbf{n}_{mb}\cdot D_m \nabla s_{mb} dA \tag{32}$$

$$a_d h_{md} = \frac{1}{V}\int_{A_{dm}} \mathbf{n}_{dm}\cdot D_d \nabla s_d dA - \frac{1}{V}\int_{A_{dm}} \mathbf{n}_{dm}\cdot \mathbf{V}_d s_d dA$$
$$= -\frac{1}{V}\int_{A_{md}} \mathbf{n}_{md}\cdot D_m \nabla s_{md} dA \tag{33}$$

Furthermore, these non-traditional convective transport terms in the closed form of macroscopic governing equations depend on the following coefficients, which are determined by

$$\mathbf{u}_b = \frac{1}{V}\int_{A_{bm}} \mathbf{n}_{bm} s_b dA - \left\langle \tilde{\mathbf{V}}_b s_b \right\rangle \tag{34a}$$

$$\mathbf{u}_{bb} = \frac{1}{V}\int_{A_{bm}} \mathbf{n}_{bm}\cdot D_b \nabla \mathbf{b}_{bb} dA - \frac{1}{V}\int_{A_{bm}} \mathbf{n}_{bm}\cdot \mathbf{V}_b \mathbf{b}_{bb} dA \tag{34b}$$

$$\mathbf{u}_{bm} = \frac{1}{V}\int_{A_{bm}} \mathbf{n}_{bm}\cdot D_b \nabla \mathbf{b}_{bm} dA - \frac{1}{V}\int_{A_{bm}} \mathbf{n}_{bm}\cdot \mathbf{V}_b \mathbf{b}_{bm} dA \tag{34c}$$

$$\mathbf{u}_{m1} = \frac{1}{V}\int_{A_{mb}} \mathbf{n}_{mb} s_{mb} dA \tag{34d}$$

$$\mathbf{u}_{m2} = \frac{1}{V}\int_{A_{md}} \mathbf{n}_{md} s_{md} dA \tag{34e}$$

$$\mathbf{u}_{mm} = \frac{1}{V}\int_{A_{mb}} \mathbf{n}_{mb}\cdot D_m \nabla \mathbf{b}_{mm} dA + \frac{1}{V}\int_{A_{md}} \mathbf{n}_{md}\cdot D_m \nabla \mathbf{b}_{mm} dA \tag{34f}$$

$$\mathbf{u}_{mb} = \frac{1}{V}\int_{A_{mb}} \mathbf{n}_{mb}\cdot D_m \nabla \mathbf{b}_{mb} dA \tag{34g}$$

$$\mathbf{u}_{md} = \frac{1}{V}\int_{A_{md}} \mathbf{n}_{md}\cdot D_m \nabla \mathbf{b}_{md} dA \tag{34e}$$

$$\mathbf{u}_d = \frac{1}{V}\int_{A_{dm}} \mathbf{n}_{dm} s_d dA - \left\langle \tilde{\mathbf{V}}_d s_d \right\rangle \tag{34i}$$

$$\mathbf{u}_{dd} = \frac{1}{V}\int_{A_{dm}} \mathbf{n}_{dm}\cdot D_d \nabla \mathbf{b}_{dd} dA - \frac{1}{V}\int_{A_{dm}} \mathbf{n}_{dm}\cdot \mathbf{V}_d \mathbf{b}_{dd} dA \tag{34j}$$

$$\mathbf{u}_{dm} = \frac{1}{V}\int_{A_{dm}} \mathbf{n}_{dm}\cdot D_d \nabla \mathbf{b}_{dm} dA - \frac{1}{V}\int_{A_{dm}} \mathbf{n}_{dm}\cdot \mathbf{V}_d \mathbf{b}_{dm} dA \tag{34k}$$

In this section, a set of upscaled solute concentration transport equations for three individual phases, namely the blood, dialysate and membrane phases, has been obtained by means of a rigorous mathematical development based on the volume averaging theory. The appearance of these macroscopic equations is similar to that of the Sano–Nakayama model, but there are a few differences between these two models indicated as below

1) There are some conductive and non-traditional convective transport terms in Eqs. (28)–(30), such as $\nabla\cdot\left[\mathbf{D}_{bm}\cdot\nabla\langle c_m\rangle^m\right]$, $\nabla\cdot\left(\mathbf{u}_b\left(\langle c_m\rangle^m-\langle c_b\rangle^b\right)\right)$ and $\mathbf{u}_{bb}\cdot\nabla\langle c_b\rangle^b$, etc., which are missing in the Sano–Nakayama model. As pointed out by Whitaker (1999), these non-traditional convective transport terms could be neglected in the case of pure diffusion in porous media. However, the contribution of these terms could be crucial when convection itself is of importance.
2) The distribution coefficient, which is in charge of interfacial mass flux distribution between two adjacent phases, is introduced into the upscaled solute concentration transport equations of countercurrent dialyzer systems for the first time.
3) In the Sano–Nakayama model, the mass transfer from the membrane to the dialysate compartment is evaluated as $\omega\langle c_m\rangle^m$. But, the mass transfer from the membrane to the dialysate compartment obtained in the present model is $\xi_{md}\omega\langle c_d\rangle^d$.

3. Solute concentration fields

In what follows, the steady one-dimensional case is treated. First, in all three concentration equations, the macroscopic diffusion terms are dropped, since such effects on the solute mass transfer would be negligibly small compared with those of the interfacial mass transfer and ultrafiltration, as pointed out by Sano and Nakayama (2012). As a consequence, the macroscopic solute concentration transport equations are reduced to

$$\frac{d}{dx}V_b\langle c_b\rangle^b = -a_b h_{mb}\left(\langle c_b\rangle^b - \langle c_m\rangle^m\right) - \xi_{mb}\omega\langle c_b\rangle^b \tag{35}$$

$$a_b h_{mb}\left(\langle c_b\rangle^b - \langle c_m\rangle^m\right) + a_d h_{md}\left(\langle c_d\rangle^d - \langle c_m\rangle^m\right) + \xi_{mb}\omega\langle c_b\rangle^b - \xi_{md}\omega\langle c_d\rangle^d = 0 \tag{36}$$

$$\frac{d}{dx}V_d\langle c_d\rangle^d = -a_d h_{md}\left(\langle c_d\rangle^d - \langle c_m\rangle^m\right) + \xi_{md}\omega\langle c_d\rangle^d \tag{37}$$

Based on Eq. (36), the membrane concentration can be obtained as

$$\langle c_m\rangle^m = \frac{a_b h_{mb}+\xi_{mb}\omega}{a_b h_{mb}+a_d h_{md}}\langle c_b\rangle^b + \frac{a_d h_{md}-\xi_{md}\omega}{a_b h_{mb}+a_d h_{md}}\langle c_d\rangle^d \tag{38}$$

which can be substituted into the solute concentration in dialysate phase Eq. (37) as

$$\frac{d}{dx}V_d\langle c_d\rangle^d = (a_d h_{md}-\xi_{md}\omega)\left(\frac{a_b h_{mb}+\xi_{mb}\omega}{a_d h_{md}+a_b h_{mb}}\langle c_b\rangle^b - \frac{a_b h_{mb}+\xi_{md}\omega}{a_d h_{md}+a_b h_{mb}}\langle c_d\rangle^d\right) + \xi_{md}\omega\langle c_m\rangle^m \tag{39}$$

The Kedem–Katchalsky model, for the case of negligible osmotic pressure, can be written as

$$\frac{d}{dx}V_d\langle c_d\rangle^d = a_b\left(P_m\left(\langle c_b\rangle^b - \langle c_d\rangle^d\right) + (1-\sigma)J_v\langle c_m\rangle^m\right) \tag{40}$$

and

$$\langle c_m\rangle^m = \left[1 - \frac{1}{Pe} + \frac{1}{\exp(Pe)-1}\right]\langle c_b\rangle^b + \left[\frac{1}{Pe} - \frac{1}{\exp(Pe)-1}\right]\langle c_d\rangle^d \tag{41}$$

where σ is the Staverman reflection coefficient (Villarroel et al., 1977) that describes how much of interfacial mass flux is reflected by membrane. In addition, P_m is the effective membrane diffusivity permeability and

$$Pe = (1-\sigma)\frac{J_V}{P_m} \tag{42}$$

For the case of very thin membranes, we can have the following relations

$$h_{md} = h_{mb} \quad \text{and} \quad \xi_{md} = \xi_{mb} \tag{43}$$

Moreover, the Staverman reflection coefficient σ can be set to be equal to the interfacial mass flux distribution coefficient in the blood phase, namely, $\xi_{bm} = 1-\xi_{mb}$. Therefore, a comparison of above two equations reveals that the Peclet number corresponds to

$$Pe = \frac{\xi_{mb}\omega(a_d h_{md}+a_b h_{mb})}{(a_d h_{md}-\xi_{mb}\omega)(a_b h_{mb}+\xi_{mb}\omega)} \tag{44}$$

which gives the following relation

$$\frac{\xi_{mb}\omega}{a_b h_{mb}} = \frac{\sqrt{1+Pe^2}-1}{Pe} \tag{45}$$

Hence, the membrane concentration can be written as

$$\langle c_m\rangle^m = \frac{\sqrt{1+Pe^2}+Pe-1}{2Pe}\langle c_b\rangle^b + \frac{Pe+1-\sqrt{1+Pe^2}}{2Pe}\langle c_d\rangle^d \tag{46}$$

For the sake of comparison, the membrane concentration based on the Sano–Nakayama model is briefly given as

$$\langle c_m\rangle^m = \frac{\sqrt{4+Pe^2}+Pe-2}{2Pe}\langle c_b\rangle^b + \frac{Pe+2-\sqrt{4+Pe^2}}{2Pe}\langle c_d\rangle^d \tag{47}$$

As presented in Fig. 3, Eq. (46) based on the present model is compared with Eqs. (47) and (41), which are obtained from the Sano–Nakayama model and the Kedem–Katchalsky model, respectively, in terms of

$$\frac{\left(\langle c_m\rangle^m - \langle c_d\rangle^d\right)}{\left(\langle c_b\rangle^b - \langle c_d\rangle^d\right)}$$

In this figure, it can be clearly seen that the agreement between the Sano–Nakayama model and the Kedem–Katchalsky model is better than that between the present model and the Kedem–Katchalsky model. However, the Sano–Nakayama model is limited to only the case of $\sigma = 0$. Considering the variation of σ, the present model is more general and practical.

In order to obtain the solute concentrations in blood and dialysate phases, substitution of Eq. (38) into the solute concentration in blood phase yields

$$\frac{d}{dx}V_b\langle c_b\rangle^b = \frac{-a_b h_{mb}(a_d h_{md}-\xi_{mb}\omega)}{a_d h_{md}+a_b h_{mb}}\left(\langle c_b\rangle^b - \langle c_d\rangle^d\right) - \xi_{mb}\omega\langle c_b\rangle^b \tag{48}$$

Since

$$V_b\langle c_b\rangle^b + V_d\langle c_d\rangle^d = V_b(1)\langle c_b\rangle^b(1) + V_d(1)\langle c_d\rangle^d(1)$$
$$= (C_V - V_d(1))\langle c_b\rangle^b(1) = const.,$$

we can have

$$\langle c_d\rangle^d = \frac{(C_V - V_d(1))\langle c_b\rangle^b(1)}{V_d} - \frac{V_b\langle c_b\rangle^b}{V_d} \tag{49}$$

where the inlet solute concentration of dialysate $\langle c_d\rangle^d(1)$ is assumed to be zero and

$$C_V = V_b + V_d = const. \tag{50}$$

Furthermore, Eqs. (48) and (49) can be combined to give

$$\frac{d}{dx}\langle c_b\rangle^b + P(x)\langle c_b\rangle^b = Q(x)\langle c_b\rangle^b(1) \tag{51}$$

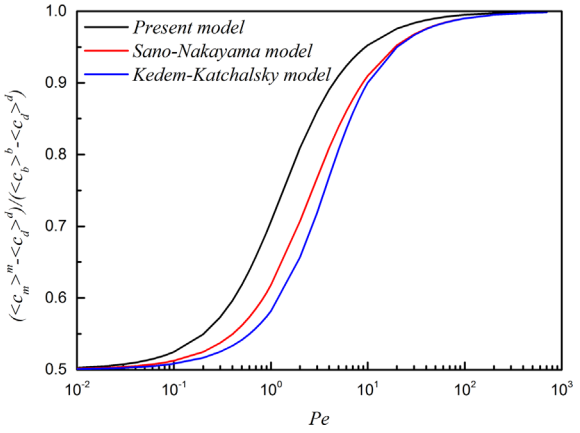

Fig. 3. Comparison of the present model, the Sano–Nakayama model and the Kedem–Katchalsky model.

where

$$P(x) = \frac{a_b h_{mb}(a_d h_{md}-\xi_{mb}\omega(x))}{a_b h_{mb}+a_d h_{md}}\frac{C_V}{V_b(x)(C_V - V_b(x))} - \frac{(1-\xi_{mb})\omega(x)}{V_b(x)} \tag{52}$$

and

$$Q(x) = \frac{a_b h_{mb}(a_d h_{md}-\xi_{mb}\omega(x))}{a_b h_{mb}+a_d h_{md}}\frac{C_V - V_d(1)}{V_b(x)(C_V - V_b(x))} \tag{53}$$

At this point, the solute concentration profile in the blood phase can be easily determined for the given inlet solute concentration $\langle c_b\rangle^b(0)$

$$\frac{\langle c_b\rangle^b(x^*)}{\langle c_b\rangle^b(0)} = \frac{e^{-f_1(x^*)}\left[e^{f_1(1)} + f_2(x^*) - f_2(1)\right]}{e^{f_1(1)} - f_2(1)} \tag{54}$$

In addition, substitution of Eq. (54) into Eq. (49) yields

$$\frac{\langle c_d\rangle^d(x^*)}{\langle c_b\rangle^b(0)} = \frac{C_V - V_d(1)}{\left[e^{f_1(1)} - f_2(1)\right][C_V - V_b(x^*)]} - \frac{V_b(x^*)e^{-f_1(x^*)}\left[e^{f_1(1)} + f_2(x^*) - f_2(1)\right]}{[C_V - V_b(x^*)]\left[e^{f_1(1)} - f_2(1)\right]} \tag{55}$$

where

$$f_1(x^*) = L\int_0^{x^*} P(x^*)dx^* = L\int_0^{x^*}\left[\frac{a_b h_{mb}(a_d h_{md}-\xi_{mb}\omega(x^*))}{a_b h_{mb}+a_d h_{md}}\frac{1}{V_b(x^*)\left(1-\frac{V_b(x^*)}{C_V}\right)} - \frac{(1-\xi_{mb})\omega(x^*)}{V_b(x^*)}\right]dx^*$$
$$= \frac{1}{Pe_m}\int_0^{x^*}\left[\left(1-\frac{\xi_{mb}\omega(x^*)}{a_d h_{md}}\right)\frac{1}{\frac{V_b(x^*)}{V_b(0)}\left(1-\frac{V_b(x^*)}{C_V}\right)} - \frac{(1-\xi_{mb})\omega(x^*)LPe_m}{V_b(x^*)}\right]dx^* \tag{56}$$

and

$$f_2(x^*) = L\int_0^{x^*} Q(x^*)e^{L\int_0^{x^*}P(x^*)dx^*}dx^*$$
$$= L\int_0^{x^*}\frac{a_b h_{mb}(a_d h_{md}-\xi_{mb}\omega(x^*))}{a_b h_{mb}+a_d h_{md}}\frac{1-\frac{V_d(1)}{C_V}}{V_b(x^*)\left(1-\frac{V_b(x^*)}{C_V}\right)}e^{f_1(x^*)}dx^*$$
$$= \frac{1}{Pe_m}\int_0^{x^*}\left(1-\frac{\xi_{mb}\omega(x^*)}{a_d h_{md}}\right)\frac{1-\frac{V_d(1)}{C_V}}{\frac{V_b(x^*)}{V_b(0)}\left(1-\frac{V_b(x^*)}{C_V}\right)}e^{f_1(x^*)}dx^* \tag{57}$$

Note that $x^* = x/L$ is the dimensionless length and L is the length of the dialyzer case, the modified Peclet number,Pe_m, is defined as

$$Pe_m = \left(\frac{1}{a_b h_{mb}} + \frac{1}{a_d h_{md}}\right)\frac{V_b(0)}{L} = \frac{V_b(0)}{a_b L P_m} \tag{58}$$

Moreover, the perfusion rate $\omega(x^*)$, the blood Darcian velocity $V_b(x^*)$ and integration constant C_V obtained by Sano and Nakayama (2012) are directly shown as follows

$$\omega(x^*) = \frac{B}{L}\frac{\left(V_b(0)-\frac{C_V}{1+\alpha}\right)\cosh(B(1-x^*)) - \left(\frac{\alpha C_V}{1+\alpha} - V_d(1)\right)\cosh Bx^*}{\sinh B} \tag{59}$$

$$V_b(x^*) = \frac{C_V}{1+\alpha} + \frac{\left(V_b(0)-\frac{C_V}{1+\alpha}\right)\sinh(B(1-x^*)) + \left(\frac{\alpha C_V}{1+\alpha} - V_d(1)\right)\sinh Bx^*}{\sinh B} \tag{60}$$

$$C_V = \frac{1+\alpha}{\alpha+\cosh B}\left[V_b(0)\left(\cosh B - \frac{\sinh B}{B}\beta\right) + V_d(1)\right] \tag{61}$$

where α is the permeability ratio $K_{d_{xx}}/K_{b_{xx}}$, B is the dimensionless parameter associated with the membrane permeability and written as below

$$B=\frac{L}{d_b}\sqrt{8\varepsilon_b\frac{K_m\left(\frac{1}{K_{b_{xx}}}+\frac{1}{K_{d_{xx}}}\right)}{\ln\left(1+\frac{2t_m}{d_b}\right)}} \tag{62}$$

and β is the dimensionless transmembrane pressure at the blood inlet and can be evaluated by means of the total ultrafiltration rate $A(V_b(0)-V_b(1))$ in many practical cases

$$\beta=\frac{B}{\sinh B}\left[\cosh B+\frac{V_d(1)}{V_b(0)}-\frac{\alpha+\cosh B}{1+\alpha}\times\left(1+\frac{V_d(1)}{V_b(0)}-\frac{A(V_b(0)-V_b(1))}{AV_b(0)}\right)\right] \tag{63}$$

Note that K_m is the intrinsic permeability, $K_{b_{xx}}$ and $K_{d_{xx}}$ are axial permeability components of blood and dialysate phases, respectively. These three parameters can be deduced as follows

$$K_m=L_p\mu d_b ln(1+2t_m/d_b)/2 \tag{64a}$$

$$K_{b_{xx}}=\varepsilon_b d_b^2/32 \tag{64b}$$

$$K_{d_{xx}}=\varepsilon_d\left(\varepsilon_d d_b^2/(\varepsilon_b d_d)\right)^2/32 \tag{64c}$$

where L_p is hydraulic permeability of the membrane and provided to estimate the intrinsic permeability in reality.

In what follows, the most important parameter in countercurrent dialyzer system, namely, the clearance of the solute from blood to dialysate CL is given by

$$\begin{aligned}CL&=A\frac{V_b(0)\langle c_b\rangle^b(0)-V_b(1)\langle c_b\rangle^b(1)}{\langle c_b\rangle^b(0)}\\&=AV_b(0)\left[1-\frac{C_V-V_d(1)}{V_b(0)}\frac{1}{e^{f_1(1)}-f_2(1)}\right]\end{aligned} \tag{65}$$

4. Results and discussion

In this section, all geometric data associated with countercurrent dialyzer system are obtained from a Hospal Filtral 12 AN69HF module. Two kinds of solute, namely creatinine and vitamin B12, are chosen to be the study objects. Regarding to the geometric characteristics of membrane module provided by the manufacturer and hydraulic properties of two solutes reported by Ding et al. (2004), detailed information are summarized in Table 1.

In order to verify the solute concentration profiles of blood and dialysate phases derived in this study, a comparison between the present and Sano–Nakayama models are conducted for the case of pure diffusion. Since the solute concentration profiles in both the blood and dialysate phases indicated in Eqs. (54) and (55) involve complex intergradations, it is difficult to obtain their explicit analytical solutions. In this study, numerical solutions are carried out with the help of the fourth-order Runge–Kutta method (Nakayama, 1995). According to the present and Sano–Nakayama models, solute concentration variations of both blood and dialysate phases along the axial coordinate for the case of pure diffusion are plotted in Fig. 4. It can be clearly seen that the agreement between these two models are fairly good. This is because for the case of pure diffusion, one has $K_m=0$. Then, the present model naturally becomes consistent with the Sano–Nakayama model.

In the forthcoming part, the effects of ultrafiltration flow rate and distribution coefficient on both solute concentration variations along the axial coordinate and clearance enhancement are investigated. As shown in Fig. 5, the solute concentration

Table 1
Geometric characteristics of membrane module and hydraulic properties of two solutes.

Parameter	Value	Parameter	Value
L	20 cm	N	8500
d_b	220 μm	t_m	45 μm
A	11.94 cm^2	a_b	4920 m^{-1}
L_p	5.63×10^{-11} m/s Pa	P_m (creatinine)	4.172×10^{-6} m/s
P_m (vitamin B12)	1.675×10^{-6} m/s		

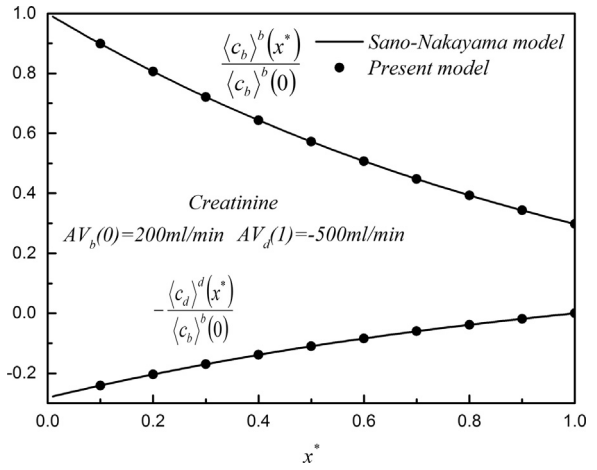

Fig. 4. Comparison of solute concentration variations along the axial coordinate of Sano–Nakayama and present models for the case of pure diffusion.

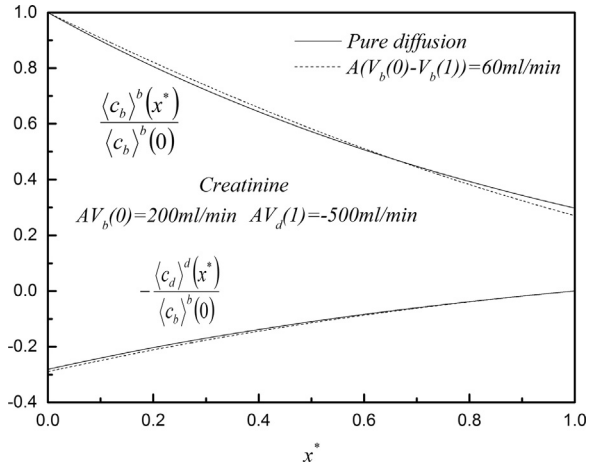

Fig. 5. Effect of ultrafiltration flow rate on solute concentration variations along the axial coordinate ($\xi_{mb}=1.0$).

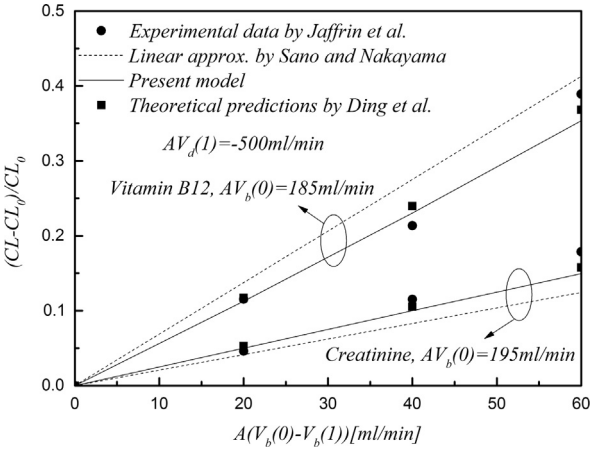

Fig. 6. Effect of ultrafiltration flow rate on the clearance enhancement ($\xi_{mb}=1.0$).

Table 2
The design and operation parameters used for comparisons in Fig. 6.

Parameter	*Value*	*Parameter*	*Value*
L	20 cm	N	8500
d_b	220 μm	t_m	45 μm
A	11.94 cm^2	a_b	4920 m^{-1}
L_p	5.63×10^{-11} m/s Pa	P_m (creatinine)	4.172×10^{-6} m/s
P_m (vitamin B12)	1.675×10^{-6} m/s	$AV_d(1)$	−500 ml/min
$AV_b(0)$ (vitamin B12)	185 ml/min	$AV_b(0)$ (creatinine)	195 ml/min

variations along the length of the dialyzer are indicated for two cases, namely, pure diffusion and ultrafiltration flow rate $A(V_b(0)-V_b(1))=60$ ml/ min. From this figure, it has been found that the influence of ultrafiltration flow rate on solute concentration variations along the axial coordinate is negligible. However, ultrafiltration flow rate has significant effect on the clearance enhancement, namely, $(CL-CL_0)/CL_0$, as depicted in Fig. 6. Note that CL_0 is the clearance for the case of pure diffusion and given by

$$CL_0 = AV_b(0)\frac{\exp\left[\left(1+V_b(0)/V_d(1)\right)/Pe_m\right]-1}{\exp\left[1+V_b(0)/V_d(1)/Pe_m\right]+V_b(0)/V_d(1)} \tag{66}$$

In Fig. 6, the clearance enhancement is plotted against the ultrafiltration flow rate with experimental data reported by Jaffrin et al. (1990), theoretical predictions conducted by Ding et al. (2004) and linear approximation proposed by Sano and Nakayama (2012). The design and operation parameters used for comparisons in Fig. 6 are illustrated in Table 2. The predicted clearance enhancement of the present model exhibits the linear relationship between $(CL-CL_0)/CL_0$ and $A(V_b(0)-V_b(1))$. Moreover, it has better agreement with both experiment and theoretical predictions than the linear approximation of Sano and Nakayama (2012) in the range of ultrafiltration flow rate studied in this paper. Nevertheless, the linear relationship can only be applied to the case of moderate ultrafiltration flow rate, since the linearity ceases to be valid for large ultrafiltration flow rate. In order to improve the accuracy of the present upscaled model, particularly in the range of large ultrafiltration flow rate, there are several possible avenues: (1) reconsider the neglected terms in the treatment of steady one-dimensional case. For the case of large ultrafiltration flow rate, the effect of non-traditional convective terms might become noticeable. (2) perform the three-dimensional analysis. Sano et al. (2014a, 2014b) conducted the three-dimensional numerical simulations for countercurrent dialyzer systems based on the Sano and Nakayama membrane model, and obtained the solute concentration fields of both dialysate and blood phases. The results indicated that the distribution of solute concentration in the radial direction is non-uniform.

Fig. 7 shows the solute concentration variations along the length of the dialyzer for three different distribution coefficients ξ_{mb}, which are 1.0, 0.5 and 0.1, respectively. For the solute concentration in the dialysate phase, there is no obvious difference observed with the variation of distribution coefficient ξ_{mb}. Yet, the effect of distribution coefficient ξ_{mb} on the solute concentration in the blood phase is discernible. In addition, the effect of distribution coefficient ξ_{mb} on the clearance enhancement are presented in Fig. 8. With the rise of distribution coefficient ξ_{mb}, the clearance enhancement for both creatinine and vitamin B12 increases linearly. It should be noted that, under the same circumstance, the clearance enhancement of the case of vitamin B12 has more strong dependence on distribution coefficient ξ_{mb} than that of the case of creatinine does. In summary, it can be concluded from Figs. 6 and 8 that clearance enhancement of countercurrent dialyzer systems would increase with the rise of ultrafiltration flow rate and distribution coefficient ξ_{mb}.

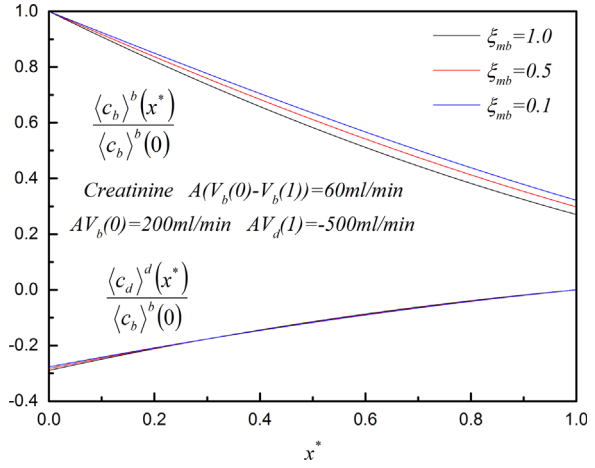

Fig. 7. Effect of distribution coefficient ξ_{mb} on solute concentration variations along the axial coordinate.

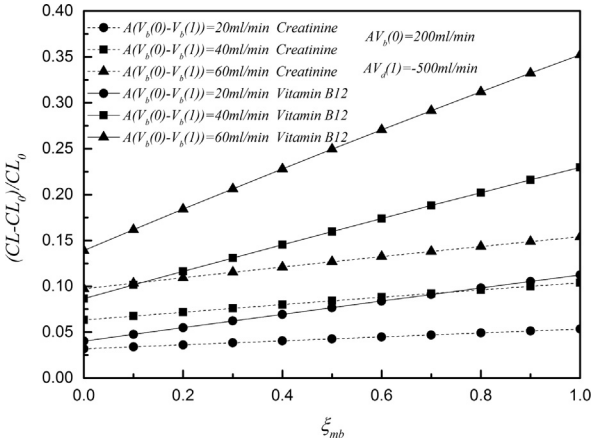

Fig. 8. Effect of distribution coefficient ξ_{mb} on the clearance enhancement.

5. Conclusions

In the present paper, a complete set of upscaling solute concentration equations for countercurrent fiber membrane dialyzer systems has been derived based on the volume averaging theory. In order to close the upscaled equations, the corresponding closure problems were given. Then, the effective coefficients existing in the upscaled equations can be achieved after solving the associated closure problems. It should be noted that the present model is similar to the Sano–Nakayama model, but it is more general and realistic due to the introduction of distribution coefficient on the basis of a rigorous mathematical development. Subsequently, the steady one-dimensional analysis has been conducted in full consideration of the macroscopic diffusion terms, so as to obtain the analytical expressions of solute concentration

distributions in both blood and dialysate phases. In order to elucidate the effects of ultrafiltration flow rate and distribution coefficient on both clearance enhancement and solute concentration variations along the axial coordinate, these analytical expressions were solved by using the Runge–Kutta–Gill method (Nakayama, 1995). Based on the results obtained in this study, several remarks can be drawn:

1) For the case of pure diffusion, the comparison between the present model and the Sano–Nakayama model was performed. Since the present model can be reduced to the Sano–Nakayama model for this simple case, the solute concentration variations along the axial coordinate of the present model is consistent with that of the Sano–Nakayama model, demonstrating the validity of the present model.
2) It was found out that ultrafiltration flow rate has no significant impact on the solute concentration variations along the length of the dialyzer. However, the clearance enhancement increases linearly with the rise of ultrafiltration flow rate. Moreover, the clearance enhancement prediction based on the present model is accordance with available experimental data and theoretical predictions, despite the case of high ultrafiltration flow rate. The present model exhibits better agreement with both experiment and theoretical predictions than the linear approximation of Sano and Nakayama (2012).
3) By varying the distribution coefficient ξ_{mb}, no obvious difference related to the solute concentration in the dialysate phase was observed. However, the impact of distribution coefficient ξ_{mb} on the solute concentration in the blood phase was noticeable. In addition, it has been found that the positive linear relationship exhibits between the clearance enhancement and distribution coefficient ξ_{mb}. It also should be noted that the clearance enhancement of the case of vitamin B12 is more sensitive to the distribution coefficient ξ_{mb} than that of the case of creatinine.

Nomenclature

a specific surface area (1/m)
A cross-sectional area of the dialyzer case (m^2)
A_{mb} interfacial surface area between the membrane and blood phases (m^2)
$\mathbf{b}$ closure variable
B dimensionless parameter associated with membrane permeability
c solute concentration (kg/m^3)
C_V integration constant (m/s)
CL clearance (m^3/s)
d diameter (m)
D solute diffusion coefficient (m^2/s)
$\mathbf{D}$ effective solute diffusion tensor (m^2/s)
$f(x^*)$ dimensionless function
h mass transfer coefficient (m/s)
$\mathbf{I}$ unit matrix
J_V ultrafiltration velocity (m/s)
K permeability (m^2)
l microscopic characteristic length (m)
L effective length of the dialyzer case (m)
L_p hydraulic permeability of membrane (m/s Pa)
$\mathbf{n}_{bm}$ normal unit vector from the blood phase to the membrane phase
N number of hollow fibers
q interfacial mass flux (kg/m^3s)
p pressure (Pa)
Pe Peclet number
Pe_m modified Peclet number
P_m effective membrane diffusivity permeability (m/s)
r radial coordinate (m) or special closure variable
r_o characteristic length associated with averaging volume (m)
s closure variable
t time (s)
t_m membrane thickness (m)
$\mathbf{u}$ transport coefficient (m/s)
V unit cell volume (m^3) or velocity (m/s)
$\mathbf{V}$ velocity tensor (m/s)
x axial coordinate (m)
x^* dimensionless axial coordinate

Greek letters

α permeability ratio
β dimensionless transmembrane pressure at the blood inlet
ε porosity
μ dynamic viscosity (Pa s)
ρ density (kg/m^3)
ω perfusion rate (1/s)
ψ arbitrary variable
ξ distribution coefficient
σ Staverman reflection coefficient

Special symbols

$\tilde{\psi}$ deviation from intrinsic average
$\langle\psi\rangle$ Darcian average
$\langle\psi_{b,d,m}\rangle^{b,d,m}$ intrinsic average

Subscripts and superscripts

b blood
c concentration
d dialysate
f fluid
m membrane

Acknowledgement

The authors would like to express their sincere thanks to the National Natural Science Foundation of China (No. 21176049) and Fuzhou University Qishan Scholar (Oversea project) (XRC-1458) for supporting this study.

Appendix

This Appendix is devoted to the resolution of closure problems. Substitution of these spatial deviation representations given by Eqs. (27a), (27b) and (27c) into macroscale unclosed solute transport Eqs. (11)–(13) leads to the governing differential equations of closure variables. The first closure problem is associated with $\nabla\langle c_b\rangle^b$ and takes the following form

Problem I: for the source term $\nabla\langle c_b\rangle^b$

$$\mathbf{V}_b\cdot\nabla\mathbf{b}_{bb}+\tilde{\mathbf{V}}_b=D_b\nabla^2\mathbf{b}_{bb}-\frac{\varepsilon_b^{-1}}{V}\int_{A_{bm}}\mathbf{n}_{bm}\cdot D_b\nabla\mathbf{b}_{bb}dA+\frac{\varepsilon_b^{-1}}{V}\int_{A_{bm}}\mathbf{n}_{bm}\cdot\mathbf{V}_b\mathbf{b}_{bb}dA \tag{67}$$

$$0 = D_m\nabla^2\mathbf{b}_{mb} - \frac{\varepsilon_m^{-1}}{V}\int_{A_{mb}}\mathbf{n}_{mb}\cdot D_m\nabla\mathbf{b}_{mb}dA - \frac{\varepsilon_m^{-1}}{V}\int_{A_{md}}\mathbf{n}_{md}\cdot D_m\nabla\mathbf{b}_{mb}dA \tag{68}$$

Boundary conditions:

$$r = d_b/2: \qquad \mathbf{b}_{bb} = \mathbf{b}_{mb} \tag{69a}$$

$$-\mathbf{n}_{bm}\cdot D_b - \mathbf{n}_{bm}\cdot D_b\nabla\mathbf{b}_{bb} + \mathbf{n}_{bm}\cdot\mathbf{V}_b\mathbf{b}_{bb} = -\mathbf{n}_{bm}\cdot D_m\nabla\mathbf{b}_{mb} \tag{69b}$$

$$\text{Periodicity}: \quad \mathbf{b}_{bb}(r+\ell_i) = \mathbf{b}_{bb}(r), \quad \mathbf{b}_{mb}(r+\ell_i) = \mathbf{b}_{mb}(r) \quad i = 1,2,3 \tag{70}$$

$$\text{Average}: \langle\mathbf{b}_{bb}\rangle^b = 0, \quad \langle\mathbf{b}_{mb}\rangle^m = 0 \tag{71}$$

Problem II: for the source term $\nabla\langle c_m\rangle^m$

$$\mathbf{V}_b\cdot\nabla\mathbf{b}_{bm} = D_b\nabla^2\mathbf{b}_{bm} - \frac{\varepsilon_b^{-1}}{V}\int_{A_{bm}}\mathbf{n}_{bm}\cdot D_b\nabla\mathbf{b}_{bm}dA + \frac{\varepsilon_b^{-1}}{V}\int_{A_{bm}}\mathbf{n}_{bm}\cdot\mathbf{V}_b\mathbf{b}_{bm}dA \tag{72}$$

$$0 = D_m\nabla^2\mathbf{b}_{mm} - \frac{\varepsilon_m^{-1}}{V}\int_{A_{mb}}\mathbf{n}_{mb}\cdot D_m\nabla\mathbf{b}_{mm}dA - \frac{\varepsilon_m^{-1}}{V}\int_{A_{md}}\mathbf{n}_{md}\cdot D_m\nabla\mathbf{b}_{mm}dA \tag{73}$$

$$\mathbf{V}_d\cdot\nabla\mathbf{b}_{dm} = D_d\nabla^2\mathbf{b}_{dm} - \frac{\varepsilon_d^{-1}}{V}\int_{A_{dm}}\mathbf{n}_{dm}\cdot D_d\nabla\mathbf{b}_{dm}dA + \frac{\varepsilon_d^{-1}}{V}\int_{A_{dm}}\mathbf{n}_{dm}\cdot\mathbf{V}_d\mathbf{b}_{dm}dA \tag{74}$$

Boundary conditions:

$$r = d_b/2: \mathbf{b}_{bm} = \mathbf{b}_{mm} \tag{75a}$$

$$-\mathbf{n}_{bm}\cdot D_b\nabla\mathbf{b}_{bm} + \mathbf{n}_{bm}\cdot\mathbf{V}_b\mathbf{b}_{bm} = -\mathbf{n}_{bm}\cdot D_m - \mathbf{n}_{bm}\cdot D_m\nabla\mathbf{b}_{mm} \tag{75b}$$

$$r = d_d/2: \mathbf{b}_{dm} = \mathbf{b}_{mm} \tag{76a}$$

$$-\mathbf{n}_{dm}\cdot D_d\nabla\mathbf{b}_{dm} + \mathbf{n}_{dm}\cdot\mathbf{V}_d\mathbf{b}_{dm} = -\mathbf{n}_{dm}\cdot D_m - \mathbf{n}_{dm}\cdot D_m\nabla\mathbf{b}_{mm} \tag{76b}$$

$$\text{Periodicity}: \mathbf{b}_{bm}(r+\ell_i) = \mathbf{b}_{bm}(r) \;\; \mathbf{b}_{mm}(r+\ell_i) = \mathbf{b}_{mm}(r) \;\; \mathbf{b}_{dm}(r+\ell_i) = \mathbf{b}_{dm}(r) \quad i = 1,2,3 \tag{77}$$

$$\text{Average}: \langle\mathbf{b}_{bm}\rangle^b = 0, \quad \langle\mathbf{b}_{mm}\rangle^m = 0, \quad \langle\mathbf{b}_{dm}\rangle^d = 0 \tag{78}$$

Problem III: for the source term $\nabla\langle c_d\rangle^d$

$$0 = D_m\nabla^2\mathbf{b}_{md} - \frac{\varepsilon_m^{-1}}{V}\int_{A_{mb}}\mathbf{n}_{mb}\cdot D_m\nabla\mathbf{b}_{md}dA - \frac{\varepsilon_m^{-1}}{V}\int_{A_{md}}\mathbf{n}_{md}\cdot D_m\nabla\mathbf{b}_{md}dA \tag{79}$$

$$\mathbf{V}_d\cdot\nabla\mathbf{b}_{dd} + \tilde{\mathbf{V}}_d = D_d\nabla^2\mathbf{b}_{dd} - \frac{\varepsilon_d^{-1}}{V}\int_{A_{dm}}\mathbf{n}_{dm}\cdot D_d\nabla\mathbf{b}_{dd}dA + \frac{\varepsilon_d^{-1}}{V}\int_{A_{dm}}\mathbf{n}_{dm}\cdot\mathbf{V}_d\mathbf{b}_{dd}dA \tag{80}$$

Boundary conditions:

$$r = d_d/2: \mathbf{b}_{dd} = \mathbf{b}_{md} \tag{81a}$$

$$-\mathbf{n}_{dm}\cdot D_d - \mathbf{n}_{dm}\cdot D_d\nabla\mathbf{b}_{dd} + \mathbf{n}_{dm}\cdot\mathbf{V}_d\mathbf{b}_{dd} = -\mathbf{n}_{dm}\cdot D_m\nabla\mathbf{b}_{md} \tag{81b}$$

$$\text{Periodicity}: \mathbf{b}_{dd}(r+\ell_i) = \mathbf{b}_{dd}(r), \mathbf{b}_{md}(r+\ell_i) = \mathbf{b}_{md}(r) \;\; i = 1,2,3 \tag{82}$$

$$\text{Average}: \langle\mathbf{b}_{dd}\rangle^d = 0, \quad \langle\mathbf{b}_{md}\rangle^m = 0 \tag{83}$$

Problem IV: for the source term $\left(\langle c_m\rangle^m - \langle c_b\rangle^b\right)$

$$\mathbf{V}_b\cdot\nabla s_b = D_b\nabla^2 s_b - \frac{\varepsilon_b^{-1}}{V}\int_{A_{bm}}\mathbf{n}_{bm}\cdot D_b\nabla s_b dA + \frac{\varepsilon_b^{-1}}{V}\int_{A_{bm}}\mathbf{n}_{bm}\cdot\mathbf{V}_b s_b dA \tag{84}$$

$$0 = D_m\nabla^2 s_{mb} - \frac{\varepsilon_m^{-1}}{V}\int_{A_{mb}}\mathbf{n}_{mb}\cdot D_m\nabla s_{mb}dA - \frac{\varepsilon_m^{-1}}{V}\int_{A_{md}}\mathbf{n}_{md}\cdot D_m\nabla s_{mb}dA \tag{85}$$

Boundary conditions:

$$r = d_b/2: \qquad s_b = s_{mb} + 1 \tag{86a}$$

$$-\mathbf{n}_{bm}\cdot D_b\nabla s_b + \mathbf{n}_{bm}\cdot\mathbf{V}_b s_b = -\mathbf{n}_{bm}\cdot D_m\nabla s_{mb} \tag{86b}$$

$$\text{Periodicity}: s_b(r+\ell_i) = s_b(r), \;\; s_{mb}(r+\ell_i) = s_{mb}(r), i = 1,2,3 \tag{87}$$

$$\text{Average}: \langle s_b\rangle^b = 0, \langle s_{mb}\rangle^m = 0 \tag{88}$$

Problem V: for the source term $\left(\langle c_m\rangle^m - \langle c_d\rangle^d\right)$

$$0 = D_m\nabla^2 s_{md} - \frac{\varepsilon_m^{-1}}{V}\int_{A_{mb}}\mathbf{n}_{mb}\cdot D_m\nabla s_{md}dA - \frac{\varepsilon_m^{-1}}{V}\int_{A_{md}}\mathbf{n}_{md}\cdot D_m\nabla s_{md}dA \tag{89}$$

$$\mathbf{V}_d\cdot\nabla s_d = D_d\nabla^2 s_d - \frac{\varepsilon_d^{-1}}{V}\int_{A_{dm}}\mathbf{n}_{dm}\cdot D_d\nabla s_d dA + \frac{\varepsilon_d^{-1}}{V}\int_{A_{dm}}\mathbf{n}_{dm}\cdot\mathbf{V}_d s_d dA \tag{90}$$

Boundary conditions:

$$r = d_d/2: s_d = s_{md} + 1 \tag{91a}$$

$$-\mathbf{n}_{dm}\cdot D_d\nabla s_d + \mathbf{n}_{dm}\cdot\mathbf{V}_d s_d = -\mathbf{n}_{dm}\cdot D_m\nabla s_{md} \tag{91b}$$

$$\text{Periodicity}: s_d(r+\ell_i) = s_d(r), \;\; s_{md}(r+\ell_i) = s_{md}(r) \; i = 1,2,3 \tag{92}$$

$$\text{Average}: \langle s_d\rangle^d = 0, \;\; \langle s_{md}\rangle^m = 0 \tag{93}$$

The final two closure problems are used to determine how the interfacial mass flux is distributed between the adjacent two phases. At the interface between the blood and membrane phases, the closure problem takes the form

Problem VI: for interfacial mass flux between blood and membrane phases q_{bm}

$$\mathbf{V}_b\cdot\nabla r_{bm} = D_b\nabla^2 r_{bm} - \varepsilon_b^{-1}a_b\xi_{bm} \tag{94}$$

$$0 = D_m\nabla^2 r_{mb} - \varepsilon_m^{-1}a_b\xi_{mb} \tag{95}$$

Boundary conditions:

$$r = d_b/2: r_{bm} = r_{mb} \tag{96a}$$

$$-\mathbf{n}_{bm}\cdot D_b\nabla r_{bm} + \mathbf{n}_{bm}\cdot\mathbf{V}_b/\omega + \mathbf{n}_{bm}\cdot\mathbf{V}_b r_{bm} = -\mathbf{n}_{bm}\cdot D_m\nabla r_{mb} \tag{96b}$$

$$\text{Periodicity}: r_{bm}(r+\ell_i) = r_{bm}(r), r_{mb}(r+\ell_i) = r_{mb}(r), \qquad i = 1,2,3 \tag{97}$$

$$\text{Average}: \langle r_{bm}\rangle^b = 0, \langle r_{mb}\rangle^m = 0 \tag{98}$$

where ξ_{bm} and ξ_{mb} are distribution coefficients given by

$$\xi_{bm} = \frac{1}{A_{bm}}\int_{A_{bm}}\mathbf{n}_{bm}\cdot D_b\nabla r_{bm}dA + \frac{1}{A_{bm}}\int_{A_{bm}}\mathbf{n}_{bm}\cdot\mathbf{V}_b r_{bm}dA \tag{99a}$$

$$\xi_{mb} = \frac{1}{A_{mb}}\int_{A_{mb}}\mathbf{n}_{mb}\cdot D_m\nabla r_{mb}dA \tag{99b}$$

Based on the interfacial boundary condition, it can be quickly concluded that the coefficients are constrained by

$$\xi_{bm} + \xi_{mb} = 1 \tag{100}$$

For the case of heterogeneous thermal source generated at the interface between two phases, Quintard and Whitaker (2000) provided the corresponding closure problem for distribution coefficient and obtained its analytical solution for a stratified system. It has been found that the thermal conductivity ratio of two phases plays an important role in determining distribution

coefficient. Related to the distribution coefficient discussed in this paper, it can be deduced by analogy that the distribution coefficient mainly depends on the diffusion coefficient ratio of blood phase to membrane phase. Moreover, based on the closure problem, the velocity at the interface also has certain influence on the distribution coefficient.

Problem VII: for interfacial mass flux between dialysate and membrane phases q_{dm}

$$0 = D_m \nabla^2 r_{md} - \varepsilon_m^{-1} a_d \xi_{md} \tag{101}$$

$$\mathbf{V}_d \cdot \nabla r_{dm} = D_d \nabla^2 r_{dm} - \varepsilon_d^{-1} a_d \xi_{dm} \tag{102}$$

Boundary conditions:

$$r = d_d/2 : r_{md} = r_{dm} \tag{103a}$$

$$-\mathbf{n}_{dm} \cdot D_d \nabla r_{dm} + \mathbf{n}_{dm} \cdot \mathbf{V}_d/\omega + \mathbf{n}_{dm} \cdot \mathbf{V}_d r_{dm} = -\mathbf{n}_{dm} \cdot D_m \nabla r_{md} \tag{103b}$$

$$\text{Periodicity} : r_{dm}(r+\ell_i) = r_{dm}(r), \quad r_{md}(r+\ell_i) = r_{md}(r) \quad i = 1,2,3 \tag{104}$$

$$\text{Average} : \langle r_{dm} \rangle^d = 0, \langle r_{md} \rangle^m = 0 \tag{105}$$

where ξ_{dm} and ξ_{md} are distribution coefficients given by

$$\xi_{dm} = \frac{1}{A_{dm}} \int_{A_{dm}} \mathbf{n}_{dm} \cdot D_d \nabla r_{dm} dA + \frac{1}{A_{dm}} \int_{A_{dm}} \mathbf{n}_{dm} \cdot \mathbf{V}_d r_{dm} dA \tag{106a}$$

$$\xi_{md} = \frac{1}{A_{md}} \int_{A_{md}} \mathbf{n}_{md} \cdot D_m \nabla r_{md} dA \tag{106b}$$

Furthermore, these two distribution coefficients are constrained by

$$\xi_{dm} + \xi_{md} = 1 \tag{107}$$

References

Bear, J., 1972. Dynamics of Fluids in Porous Media. Elsevier, New York, NY.

Cooney, D.O., Kim, S.S., Davis, E.J., 1974. Analyses of mass transfer in hemodialyzers for laminar blood flow and homogeneous dialysate. Chem. Eng. Sci. 29, 1731–1738.

Davit, Y., Wood, B.D., Debenest, G., Quintard, M., 2012. Correspondence between one-and two-equation models for solute transport in two-region heterogeneous porous media. Transp. Porous Media 95 (1), 213–238.

Ding, W.P., He, L.Q., Zhao, G., Zhang, H.F., Shu, Z.Q., Gao, D.Y., 2004. Double porous media model for mass transfer of hemodialyzers. Int. J. Heat Mass Transfer 47, 4849–4855.

Gray, W.G., 1975. A derivation of the equations for multi-phase transport. Chem. Eng. Sci. 30 (2), 229–233.

Jaffrin, M.Y., Ding, L., Laurent, J.M., 1990. Simultaneous convective and diffusive mass transfer in a hemodialyzer. J. Biomech. Eng. 112, 212–219.

Krogh, A., 1919. The number and distribution of capillaries in muscles with calculations of the oxygen pressure head necessary for supplying the tissue. J. Physiol. 52, 409–415.

Kedem, O., Katchalsky, A., 1958. Thermodynamics analysis of the permeability of biological membranes to non-electrolytes. Biochim. Biophys. Acta 27, 229–246.

Kumar, V., Upadhyay, S.N., 2000. Computer simulation of membrane processes: ultrafiltration and dialysis units. Comput. Chem. Eng. 23, 1713–1724.

Labecki, M., Piret, J.M., Bowen, B.D., 1995. Two-dimensional analysis of fluid flow in hollow-fibre modules. Chem. Eng. Sci. 50 (21), 3369–3384.

Lu, J.F., Lu, W.Q., 2010. A numerical simulation for mass transfer through the porous membrane of parallel straight channels. Int. J. Heat Mass Transfer 53, 2404–2413.

Moyne, C., 1997. Two-equation model for a diffusive process in porous media using the volume averaging method with an unsteady-state closure. Adv. Water Resour. 20 (2), 63–76.

Nakayama, A., 1995. PC-aided Numerical Heat Transfer and Convective Flow. CRC Press, Boca Raton, FL.

Nakayama, A., Sano, Y., 2013. An application of the Sano–Nakayama membrane transport model in hollow fiber reverse osmosis desalination systems. Desalination 311, 95–102.

Palatý, Z., Zakova, A., Petrik, P., 2006. A simple treatment of mass transfer data in continuous dialyzer. Chem. Eng. Process. 45, 806–811.

Quintard, M., Whitaker, S., 1993. One-and two-equation models for transient diffusion processes in two-phase systems. Adv. Heat Transfer 23 (C), 369–464.

Quintard, M., Whitaker, S., 2000. Theoretical analysis of transport in porous media. In: Hadim, H., Vafai, K. (Eds.), Handbook of Heat Transfer in Porous Media. Marcel Decker, Inc., New York, NY, pp. 1–52.

Sano, Y., Nakayama, A., 2012. A porous media approach for analyzing a counter-current dialyzer system. ASME Trans J. Heat Transfer 134 (7), 072602.

Sano, Y., Adachi, J., Nakayama, A., 2013. A porous media theory for characterization of membrane blood oxygenation devices. Heat Mass Transfer 49, 973–984.

Sano, Y., Nishimura, T., Nagase, K., 2014a. A porous media approach for hollow fiber transport phenomena. Open J. Heat, Mass Momentum Transfer 2, 11–27.

Sano, Y., Horibe, A., Haruki, N., Nagase, K., Nakayama, A., 2014b. Numerical approach for optimal design of a hollow fiber dialyzer system. Open J. Heat, Mass Momentum Transfer 2, 58–69.

Shirazian, S., Moghadassi, A., Moradi, S., 2009. Numerical simulation of mass transfer in gas–liquid hollow fiber membrane contactors for laminar flow conditions. Simul. Modell. Pract. Theory 17, 708–718.

Tu, J.W., Ho, C.D., 2010. Two-dimensional mass-transfer model of a flat-plate dialyzer with ultrafiltration operation. Chem. Eng. Technol. 33 (8), 1358–1368.

Tu, J.W., Ho, C.D., Yeh, H.M., 2006. The analytical and experimental studies of the parallel-plate concurrent dialysis system coupled with ultrafiltration. J. Membr. Sci. 281, 676–684.

Tu, J.W., Ho, C.D., Chuang, C.J., 2009. Effect of ultrafiltration on the mass-transfer efficiency improvement in a parallel-plate countercurrent dialysis system. Desalination 242, 70–83.

Villarroel, F., Klein, E., Holland, F., 1977. Solute flux in hemodialysis and hemofiltration membranes. Trans. Am. Soc. Artif. Intern. Organs 23 (1), 225–232.

Wang, Y., Brannock, M., Cox, S., Leslie, G., 2010. CFD simulations of membrane filtration zone in a submerged hollow fiber membrane bioreactor using a porous media approach. J. Membr. Sci. 363, 57–66.

Waniewski, J., 2006. Mathematical modelling of fluid and solute transport in hemodialysis and peritoneal dialysis. J. Membr. Sci. 274, 24–37.

Whitaker, S., 1999. The Method of Volume Averaging. Kluwer Academic Publishers, Dordrecht.